Research Article

Journal of PeptideScience

Received: 7 January 2012 Revised: 1 February 2012 Accepted: 17 February 2012 Published online in Wiley Online Library: 17 May 2012

(wileyonlinelibrary.com) DOI 10.1002/psc.2407

Cysteine racemization during the Fmoc solid phase peptide synthesis of the Nav1.7-selective peptide – protoxin II

Jae H. Park,* Kevin P. Carlin, Gang Wu, Victor I. Ilyin and Donald J. Kyle

Protoxin II is biologically active peptide containing the inhibitory cystine knot motif. A synthetic version of the toxin was generated with standard Fmoc solid phase peptide synthesis. If *N*-methylmorpholine was used as a base during synthesis of the linear protoxin II, it was found that a significant amount of racemization (approximately 50%) was observed during the process of cysteine residue coupling. This racemization could be suppressed by substituting *N*-methylmorpholine with 2,4,6-collidine. The crude linear toxin was then air oxidized and purified. Electrophysiological assessment of the synthesized protoxin II confirmed its previously described interactions with voltage-gated sodium channels. Eight other naturally occurring inhibitory knot peptides were also synthesized using this same methodology. The inhibitory potencies of these synthesized toxins on Nav1.7 and Nav1.2 channels are summarized. Copyright © 2012 European Peptide Society and John Wiley & Sons, Ltd.

Keywords: Nav1.7; air oxidation; 2,4,6-collidine; electrophysiology; ND7/23; patch clamp; ProTx II; PaTx I; PaTx II; GsMTx II; GrTx I; VsTx II; GsAF I; GsAF II; JzTx V; JzTx XII

Introduction

Mammalian voltage-gated sodium channels (VGSC) are composed of a large pore-forming α-subunit and two auxiliary β-subunits that are presumed to modulate channel activity and functional expression in cell membranes. Each α-subunit has four domains (D1–D4), with each domain containing six transmembrane segments (S1-S6). Nine different isoforms of the α-subunit have been described (Nav1.1–Nav1.9), with the Nav1.4 isoform being mainly expressed in skeletal muscle and the Nav1.5 isoform being mainly expressed in cardiac tissue. The remaining seven isoforms are expressed in neurons, with Nav1.7, Nav1.8 and Nav1.9 being predominantly expressed in the peripheral nervous system [1]. Nav1.7 channels exhibit slow closed-state inactivation, meaning they can respond to slow membrane depolarization [2]. As a result, Nav1.7 channels may act to amplify small excitatory inputs that are close to the resting potential, thus participating in the spontaneous action potentials in DRG neurons during pathological firing [3]. In addition to this mechanistic evidence for Nav1.7 in pain signaling, an impaired response to inflammatory pain stimuli has been described in mice in which Nav1.7 channels have been knocked out in a subset of peripheral nociceptors [4]. In humans, certain nonsense mutations in the SCN9A gene on chromosome 2q24.3 (that encodes the Nav1.7 α-subunit) have been associated with a phenotype unable to perceive certain noxious stimuli, although other sensory perceptions are normal [5]. Other mutations of the human SCN9A gene cause impairment of normal inactivation of the Nav1.7 channel, causing a persistent painful hereditary condition known as paroxysmal extreme pain disorder. A third pathophysiological condition that is hereditarily linked to mutations in the SCN9A gene is primary erythromelalgia. The mutations underlying this condition cause channels to activate at a lower membrane potential, and clinically this condition manifests as severe burning pain in the extremities [1]. Taken together, these mechanistic and behavioral observations have fueled interest in Nav1.7 channels as an important new drug target for treating various human pain conditions. For the purpose of alleviating pain without adverse side effects that are common in existing therapies, the development of a Nav1.7 channel-selective antagonist may be an attractive alternative approach. One strategy for the design of new molecules that are intended to have inherent target specificity is to initiate structure–activity relationship (SAR) studies on key natural products that are known to already exhibit some degree of the desired target specificity. The goal is to optimize the pharmaceutical profile of the molecule in parallel with optimization of the target specificity, while at the same time simplifying the molecular structure. The most Nav1.7 isoform-selective, natural product molecule described to date is protoxin II, making it a candidate for this medicinal chemistry strategy.

* *Correspondence to: Jae H. Park, Discovery Research, Purdue Pharma LP, 6 Cedar Brook Drive, Cranbury, NJ 08512, USA. E-mail: JaeHyun.Park@Pharma.com*

Discovery Research, Purdue Pharma LP. 6 Cedar Brook Drive, Cranbury, NJ, 08512, USA

Abbreviations used: *Boc, tert*-butyloxycarbonyl; Fmoc, fluorenylmethyl oxycarbonyl; DCM, dichloromethane; DIPEA, *N,N*-diisopropylethylamine; DMEM, Dulbecco's modified Eagle medium; DMF, *N,N*-dimethylformamide; EGTA, ethylene glycol tetra-acetic acid; GSH, reduced L-glutathione; GSSG, oxidized (−)-glutathione; HCTU, 2-(6-chloro-1H-benzotriazole-1-yl)-1,1,3,3-tetramethylaminium hexafluorophosphate; HEPES, (4-(2-hydroxyethyl)-1-piperazineethanesulfonic acid); NMM, *N*-methylmorpholine; Pbf, pentamethyldihydrobenzofuran-5-sulfonyl; tBu, *tert*-butyl; TFA, trifluoroacetic acid; TIS, triisopropylsilane; Trt, triphenylmethyl; Tris–HCl, Trizma® hydrochloride.

Journal of PeptideScience

Protoxin II is a naturally occurring toxin isolated from venom of the tarantula, *Thrixopelma pruriens* [6]. This toxin has been shown to selectively inhibit Nav1.7 channels approximately 100-fold more potently than other Nav isoforms [7]. Protoxin II has 30 amino acids (YCQKW MWTCD SERKC CEGMV CRLWC KKKLW) and contains six cysteine (Cys) residues, which participate in three disulfide bonds that largely stabilize an overall tertiary conformation that is essential for its Nav1.7 channel-mediated pharmacology and specificity. This pattern of disulfide bonds is characteristic of several related toxins that are usually inhibitory when occupying their respective target ion channels and is referred to as an 'inhibitory cystine knot' motif [8]. The bridging pattern is Cys1–Cys4, Cys2–Cys5 and Cys3–Cys6.

Cysteine residues are known to racemize during coupling in Fmoc solid phase peptide synthesis (Fmoc-SPPS) [9–14], and this problematic issue is even more complex when synthesizing toxins from venomous animals because of the complex arrangement of multiple disulfide bonds. There are numerous reports on the Fmoc-SPPS of naturally occurring inhibitory cystine knot peptides such as protoxin II [15–22], but interestingly, none of these previous publications mention the extent (or lack thereof) of cysteine racemization and thus create possible ambiguity regarding the chiral purity of the reported peptides. Given that each cysteine may racemize (5–50%) during the synthetic process, the desired crude linear toxin may only comprise a small fraction of the crude product, making it difficult to isolate and subsequently purify. To improve the overall synthetic yield, simplify the purification process, lower the required time and cost and thus enable this approach to SAR studies, it is critical to minimize cysteine racemization during synthesis of the linear toxin. There are reports that cysteine racemization in non-cystine knot peptides can be minimized by changing conditions such as coupling reagents, solvents and bases [9–14].

In this report, we describe how standard conditions of Fmoc-SPPS caused racemization during linear protoxin II synthesis. Second, we describe modified synthesis conditions that minimize the cysteine racemization. Third, we demonstrate the generality of these new conditions by using them to synthesize several related cystine knot peptides, and finally using standard manual patch-clamp electrophysiology techniques, we report the channel pharmacology of this representative family of toxins as a start point for additional follow-up medicinal chemistry research aimed at the design and synthesis of Nav1.7 channel-selective inhibitors.

Materials and Methods

Materials

The side chain protecting groups for amino acids are tBu for aspartic acid, glutamic acid, serine, threonine and tyrosine; Trt for cysteine and glutamine; Pbf for arginine; Boc for lysine and tryptophan. All of orthogonally protected amino acids were purchased from Protein Technologies, Inc. (Tucson, AZ, USA), Anaspec (Fremont, CA, USA) and Chem Impex (Wooddale, IL, USA). HCTU was purchased from Protein Technologies, Inc. and Anaspec, H-Trp(Boc)-2-Cl-Trt resin (0.42 mmol/g) was purchased from Bachem (Torrence, CA, USA). Fmoc-Ile-Wang LL resin (0.29 mmol/g), Fmoc-Leu-Wang LL resin (0.24 mmol/g), Fmoc-Gly-Wang LL resin (0.35 mmol/g) and H-Met-2-Cl-Trt resin (0.64 mmol/g) were purchased from Novabiochem (Gibbstown, NJ, USA). NMM, DIPEA, piperidine, DMF, DCM, 2,4,6-collidine, TFA, TIS, 3,6-dioxa-1,8-octanedithiol, thioanisole, phenol, 0.1% TFA in acetonitrile and 0.1% TFA in water were purchased from Sigma-Aldrich (St. Louis, MO, USA).

Linear Peptide Synthesis

Linear peptide was synthesized on a Pioneer peptide synthesizer (Applied Biosystems, Carlsbad, CA, USA) and peptides were assembled stepwise on 0.05–0.1 mmol using sixfold to eightfold excess of Fmoc amino acids. Fmoc protecting group was removed using 20% piperidine in DMF and free amine was coupled with amino acids/HCTU/2,4,6-collidine in DMF/DCM (1 : 1).

Linear peptide was treated with TFA : TIS : 3,6-dioxa-1,8-octanedithiol : thio-anisole : phenol : H_2O (81.5 : 1 : 2.5 : 5 : 5 : 5 by vol.) for 2–3 h at room temperature to cleave from the resin. Cleaved peptide was treated with cold diethyl ether to precipitate peptide out, and precipitated peptide was washed with diethyl ether for three times. Crude linear peptide was purified by reversed Prep-HPLC and white solids were obtained.

Air Oxidation

GSH (0.15 mM) and GSSG (0.3 mM) were added to the mixture of urea (2 M) and Tris–HCl (0.1 M) in Milli-Q water (1 mg of peptide/10 ml; EMD Millipore Corporation, Billerica, MA, USA). pH was then adjusted to 8 using sat. aq. $NaHCO_3$. A solution of crude linear toxins in water was added then stirred for 24–48 h at room temperature. Once the reaction is completed, pH of the reaction mixture was adjusted to 3 and purified by Prep-HPLC. Generally, 5–10 mg (3–6% overall yield) of toxins were isolated after purifications.

Peptide Analysis

Crude and purified peptides were analyzed using an Agilent 1100 series LC or LC-MS, equipped with a SymmetryShield™, RP18, 5 μm, 4.6 × 150 mm column (Waters, Milford, MA, USA). Depending on the availability of the instruments, two gradients were used 10–60%B over 30 min with a flow of 1 ml/min. Buffer A was 0.1% TFA in water and Buffer B was 0.1% TFA in acetonitrile. Detection was at 220 nm. Peptide mass was analyzed with low resolution electrospray ionization.

Electrophysiology

Cells

The Nav1.2 cell line was engineered in-house, whereas the Nav 1.5 and 1.7 cell lines were subcloned from in-licensed cell lines. The human Nav1.7 isoform as well as the rat Nav1.2 isoform was expressed in HEK-293 cells whereas the human Nav1.5 isoform was expressed in CHO cells. ND7/23 cells were obtained from the European Collection of Cell Cultures. These cells were subcloned to maximize the expression of protoxin II-sensitive current. All cells were plated on 35 mm culture dishes pre-coated with poly-D-lysine in standard DMEM culture media and incubated in a 5% CO_2 incubator at 37°C. Electrophysiological recordings were made from the cultured cells approximately 12–48 h after plating.

Electrophysiology

On the day of experimentation, the 35 mm dish was placed on the stage of an inverted microscope equipped with a superfusion system that continuously perfused the culture dish with fresh

recording media. A gravity-driven fast delivery perfusion system was used to apply protoxin II directly to the cell under evaluation. This system consists of a linear array of glass pipettes connected to a motorized horizontal translator. The outlet of this fast perfusion system was positioned approximately 100 μm apart from the cell of interest.

Sodium currents were recorded in the whole-cell patch clamp configuration using an Axopatch 200B amplifier (Molecular Devices, Sunnyvale, CA, USA), 1322A A/D converter (Molecular Devices) and pClamp software (v.8; Molecular Devices). Borosilicate glass pipettes had resistance values between 1.5 and 3.0 MΩ when filled with pipette solution. Series resistance (<5 MΩ) was compensated 75–80%. Signals were sampled at 10–50 kHz and low pass filtered at 3–10 kHz.

Currents were elicited from a holding potential between −120 and −110 mV using a repetitive test pulse between 2 and 10 ms in duration. The size of the test pulse was determined on a cell-by-cell basis and was chosen to generate the maximal current amplitude. However, a fixed size of the test pulse was used on a given cell throughout the experiment.

Estimated IC50 values were generated by fitting the concentration–response data with the following equation in GraphPad Prism 5 software (La Jolla, CA, USA).

$$Y = Bottom + (Top - Bottom)/\{1 + 10\text{^}[(\mathrm{Log}IC50 - X) * HillSlope]\}$$

The top, bottom and hillslope values were constrained to 1, 0 and −1, respectively.

Solutions

To record sodium currents, the pipette solution contained (in mM) CsF (140), NaCl (10), HEPES (10), EGTA (1); pH 7.3. To record rNav1.2, hNav1.7 and sodium currents in ND7/23 cells, the recording chamber was continually perfused with Hanks Balanced Salt Solution (Invitrogen, Carlsbad, CA, USA) supplemented with 10 mM HEPES. The Hanks solution contained (in mM) $CaCl_2$ (1.26), $MgCl_2$-$6H_2O$ (0.493), $MgSO_4$-$7H_2O$ (0.407), KCl (5.33), KH_2PO_4 (0.441), NaCl (137.93), Na_2HPO_4 (0.338), glucose (5.56), pH 7.4. To record hNav1.5 sodium currents, a 'low-Na' external solution was used to reduce the amplitude of the currents. This solution contained (in mM) NaCl (78), Choline Cl (75), KCl (5.4), CaCl2 (1.8), MgCl2 (1), HEPES (5), glucose (10), pH 7.4.

Result and Discussion

Synthesis of Linear Protoxin II

The synthesis of inhibitory cystine knot peptides such as protoxin II requires two main steps. First, linear peptide synthesis followed by disulfide bridge formation among six cysteine residues. Smith *et al.* [23] reported results from an alanine scan of protoxin II and the biological activity of the resultant peptides on Nav1.5 channels. However, some linear protoxin II analogs were synthesized by recombinant expression and others were purchased, so no data on their chemical synthetic methodology were provided. One report [6] on the chemical synthesis of linear protoxin II used Boc-SPPS but did not report any cysteine racemization. Because Boc-SPPS requires TFA in every Boc deprotection and requires special teflon apparatus when cleaving peptide from the resin with HF, it was decided to synthesize linear peptide in the present study with Fmoc-SPPS. Because there have been many reports on Fmoc-SPPS of multiple cysteine-containing peptides without cysteine racemization, standard coupling reagents (HCTU and NMM in DMF) were used to synthesize linear protoxin II. When crude linear peptide was analyzed after cleavage from the resin, multiple peaks were observed in the LC/MS analysis (Figure 1A). It was difficult to analyze each peak because the individual peaks were indistinguishable. However, the area under the multiple peaks showed a similar mass of 3833.6 *m/z* ($(M+4H)^{4+}$, calc: 3833). These data indicated the possibility that the racemization had occurred during the cysteine coupling process. To determine the degree of racemization, a small fragment from the *C*-terminus of protoxin II (WCKKKLW) was synthesized under the same conditions. According to of crude fragment (Figure 1B), two peaks with the same mass of 990.5 *m/z* ($(M+H)^{+}$, calc: 991.25) were observed. This clearly demonstrated about 53% of racemization has occurred during cysteine coupling. We also concluded that during the linear protoxin II synthesis, similar degree of cysteine racemization occurred to give poor crude linear protoxin II purity.

On the basis of the report by Han *et al.* [10], changing solvent from DMF to DCM/DMF (1 : 1) and base from NMM to 2,4,6-collidine suppressed racemization during cysteine coupling. Therefore, the same fragment (WCKKKLW) was resynthesized with 2,4,6-collidine as a base and DCM/DMF (1 : 1) as a solvent. After changing solvent and base, we only observed 5% of cysteine racemization to give crude fragment with about 95% peptide purity (Figure 1C). After successful synthesis of this fragment with minimal racemization, linear protoxin II was resynthesized under these modified conditions (HCTU and 2,4,6-collidine in DMF/DCM = 1 : 1). According to LC-MS, the crude linear protoxin II purity increased significantly (Figure 1D) and the major peak had the correct mass of 3832.5 *m/z* ($(M+3H)^{3+}$, calc: 3833).

Linear protoxin II was synthesized again with HCTU in DMF/DCM (1 : 1), but this time NMM was used instead of 2,4,6-collidine to see if the solvent (DMF and DCM mixture) itself could suppress racemization. On the basis of LC/MS analysis after cleavage, the crude linear peptide had very similar HPLC trace to Figure 1A, indicating that the base itself is critical in minimizing racemization.

Air Oxidation

After obtaining a racemization-minimized crude linear protoxin II, crude peptide was then air oxidized to form disulfide bridges. When disulfides are in the Cys1–Cys4, Cys2–Cys5 and Cys3–Cys6 bridging pattern, air oxidation is a robust method [15–22] to form these disulfide bridges with high yield. Steiner and Bulaj [24] reported a summary of oxidative folding conditions in which it was observed that a pH of 6–8 was optimal and the ratio between reduced and oxidized glutathione does not significantly affect the efficiency. Therefore, the crude linear protoxin II was treated with redox reagent (2 M Urea, 0.1 M Tris–HCl, 0.15 mM GSH and 0.3 mM GSSG at pH 8.0) for 24 h and purified (Figure 1E and F). Purified protoxin II has an observed mass of 3824.4 *m/z* (calc: 3827, obsd $(M+4H)^{4+}$: 957.1) and was tested by electrophysiology.

Biological Activity of the Synthesized Protoxin II

The success of the synthesis method was tested by electrophysiologically evaluating the activity of the toxin on voltage-gated sodium channels. The hallmark of protoxin II function is its ability

Journal of PeptideScience

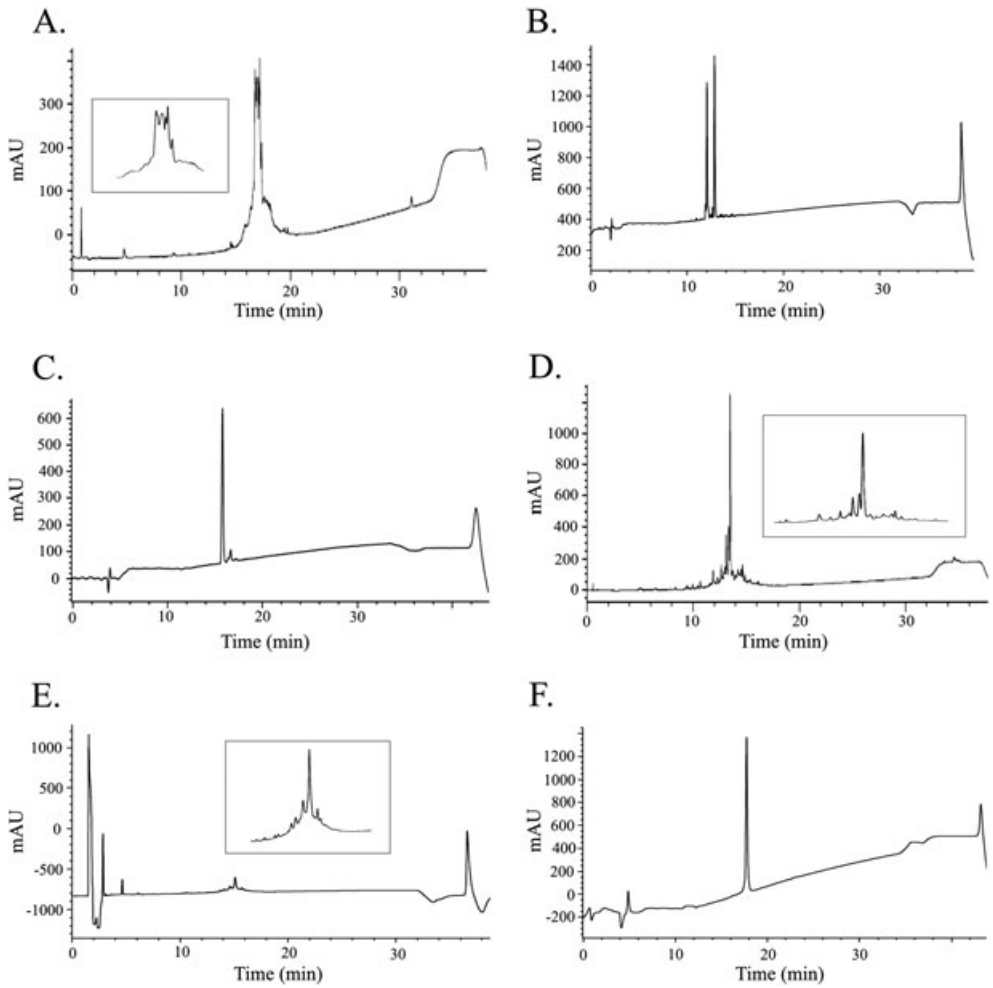

Figure 1. HPLC traces of crude peptides: (A) crude linear protoxin II with HCTU/NMM as a coupling reagent and DMF as a solvent. Enlarged chromatogram is in the box. (B) Crude protoxin II fragment, WCKKKLW with HCTU/NMM as a coupling reagent and DMF as a solvent; (C) crude protoxin II fragment, WCKKKLW with HCTU/2,4,6-collidine as a coupling reagent and DMF/DCM (1 : 1) as a solvent; (D) crude linear protoxin II with HCTU/2,4,6-collidine as a coupling reagent and DMF/DCM (1 : 1) as a solvent; (E) reaction mixture of air oxidation after 24 h. Enlarged chromatogram is in the box. (F) Purified protoxin II.

to more potently inhibit the Nav1.7 isoform of sodium channels compared with other sodium channel subtypes [7,23]. Here we present data demonstrating that the synthesized toxin was ~100-fold more potent at inhibiting the hNav1.7 current than at inhibiting the rNav1.2 and hNav1.5 mediated currents. In addition to this Nav1.7 subtype selective nature, the interaction of protoxin II with the various subtypes of voltage-gated sodium channels has many other identifying characteristics.

In Figure 2A, application of 3 nM of the synthesized toxin inhibited approximately 80% of the hNav1.7 current; this is similar to potency ascribed to the protoxin II fraction isolated from venom [6]. The binding of the toxin to the Nav.17 channel subtype and the subsequent inhibition of its current were observed to be quite slow as previously described [6,7]. This rate of current inhibition with the Nav1.7 channel subtype (Figure 2A and B) was obviously slower than the rate of current inhibition seen with both the Nav1.2 (Figure 2C) and Nav1.5 (Figure 2D) subtypes. In fact, it is this very slow inhibition of the current that did not permit us to generate a full concentration–response curve. Furthermore, the ability to unbind or 'washout' from the channel was different for Nav1.7 compared with the other subtypes tested. This feature was also noted with the native toxin [6]. As can be seen in Figure 2 when comparing panel A with panels C and D, the toxin appeared to dissociate from the Nav1.7 channel much slower than from the Nav1.2 and Nav1.5 channels – where the current amplitude was completely restored within a few minutes after removing the toxin [23,25]. In contrast, the Nav1.7 current was only partially restored after washout for an approximately tenfold longer period (Figure 2A). It was noted that a greater portion of the Nav1.7 current could recover if the cell was depolarized for a period. In the example illustrated in Figure 2B, while still in the presence of the toxin, the cell was depolarized to +50 mV for a period of 2 min that resulted in the recovery of approximately 60% of the current. Because the channels were still exposed to the toxin in this experiment, the channels again were inhibited with a slow time course. This ability to dissociate the toxin from the channel with depolarization is consistent with protoxin's proposed voltage-sensor trapping mechanism of action [26], where the binding of the toxin affects the ability of the voltage sensor to move into its outward position [7] causing a large rightward shift in the channel's voltage-dependence of activation. Depolarization is then thought to force the movement of the voltage sensor into the outward position and 'kicks off' the toxin from the channel.

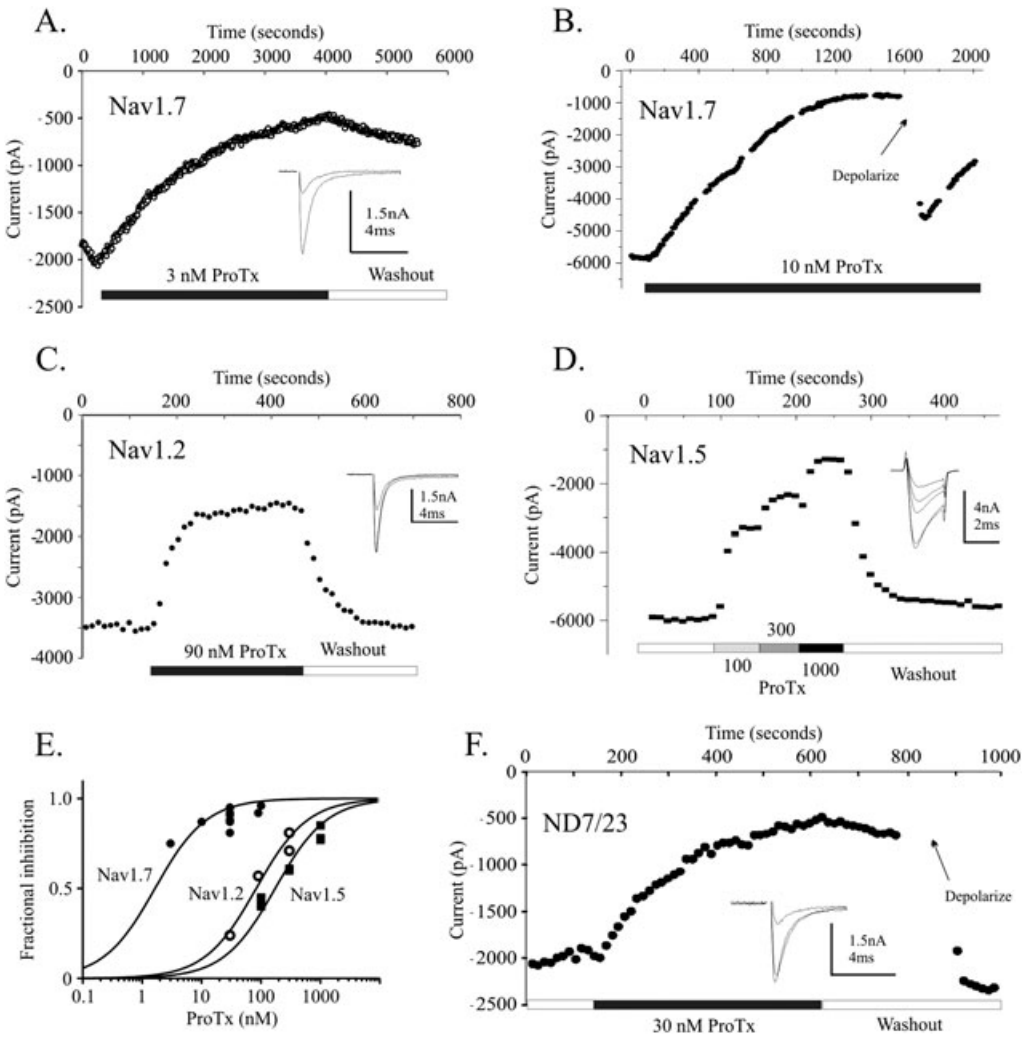

Figure 2. Biological activity of synthesized protoxin II. (A) Application of 3 nM toxin produces a slow but strong inhibition of hNav1.7 channels that are resistant to washout. Note that at this concentration the toxin required approximately 1 h to reach pseudo steady-state. Inset – overlaid raw current traces taken prior to and at fully established inhibition by the toxin. (B) The inhibition of the hNav1.7 mediated current by 10 nM toxin can be relieved by depolarizing the cell membrane at the time point indicated by the arrow. In this cell, the membrane was depolarized to +50 mV for 2 min. Current–voltage relationship data were collected at time points where data are absent. (C) rNav1.2-mediated current is less sensitive to protoxin II than the hNav1.7-mediated current. At the same time, the rates of block and recovery from block are much faster. Inset – overlaid raw current traces taken before toxin application, at the peak of inhibition and during washout. (D) The toxin shows less potent inhibition of the hNav1.5-mediated current compared with the hNav1.7-mediated current. Note that 1 μM toxin produced a similar amount of inhibition of hNav1.5 channels as 10 nM on hNav1.7 channels (compare panels B and D). Inset – overlaid raw current traces taken prior to toxin application, after application of 100 nM, 300 nM and 1 μM toxin and after washout of the toxin. (E) Concentration–response curves demonstrating the potency of the synthesized protoxin II on rNav 1.2 and hNav1.5 channels (IC50 ~80–100 nM). Compared with the partial concentration–response curve generated with hNav1.7 channels, the toxin is ~100-fold selectivity for the Nav1.7 isoform (IC50 ~ 1 nM). Each data point represents a measurement at a single concentration (hNav1.7 – filled circles ($n = 12$), rNav1.2 – open circles ($n = 4$), hNav1.5 – filled squares ($n = 9$)). (F) Synthetic protoxin II potently inhibits the native sodium current in ND7/23 cells. Inhibition and relief from block are relatively slow. Channel block was relieved by a period of membrane depolarization (0 mV holding potential with depolarizing pulse to +90 mV). Inset – raw current traces demonstrating the inhibition by 30 nM toxin compared with control and washout conditions.

Previous studies have also demonstrated the ability of membrane depolarization to restore control conditions after protoxin II application [23,25].

There was no obvious effect of the toxin on current inactivation kinetic (Figure 2A inset). This is consistent with the initial report on the native toxin [6] and recombinant toxin [25] but is opposite to the later report using Xenopus oocytes [27].

Figure 2E illustrates the Nav1.7-selective nature of the synthetic toxin. The fitted concentration–response data indicate that the IC50 on rNav1.2 and hNav1.5 channels is approximately 100 nM compared with an IC50 ~1 nM on hNav1.7 channels. This degree of Nav1.7 selectivity over Nav1.2 and Nav1.5 channels is similar to that reported for recombinant [23] and synthetic [7] versions of the toxin.

Finally, the synthesized protoxin was tested in ND7/23 cells for its ability to inhibit endogenous (non-recombinant) sodium channels. Here we demonstrate that 30 nM of the toxin was able to inhibit a large portion of the evoked current. The block of the current was relatively slow, as was the washout of the toxin. Depolarization of the cell to 0 mV, in combination with depolarizing pulses to +100 mV, was able to kick the toxin off the channels for a complete recovery of the current amplitude (Figure 2F).

Journal of PeptideScience

Table 1. Summary of nine inhibitory cystine knot peptides and their biological activities on Nav1.7 and Nav1.2

Abbreviation[a]	Sequence[b]	Mass		Retention time (min)[c]	IC50 (nM)		Folds[d]	Reference
		Calculated	Observed		Nav1.7	Nav1.2		
ProTx II	YCQKWMWTCDSERKCCEGMVCRLWCKKKLW	3826.66	3826.8 $[M+3H]^{3+}$	15.3	1 ± 0	105 ± 20	105	[6]
JzTx V	YCQKWMWTCDSKRACCEGLRCKLWCRKII	3606.41	3605.6 $[M+4H]^{4+}$	14.1	14 ± 10	157 ± 20	11	[28]
JzTx XII	YCQKWMWTCDSERKCCEGYVCELWCKYNL	3666.29	3666.9 $[M+3H]^{3+}$	15.8	1,527 ± 130	73,939 ± 14,440	48	[29]
GsAF I	YCQKWLWTCDSERKCCEDMVCRLWCKKRL	3708.46	3709.2 $[M+3H]^{3+}$	16.8	249 ± 20	255 ± 43	1	[30,31]
GsAF II	YCQKWMWTCDEERKCCEGLVCRLWCKKKIEW	3979.78	3979.2 $[M+4H]^{4+}$	15.7	70 ± 10	410 ± 20	6	[30,31]
VsTx II	YCQKWMWTCDEERKCCEGLVCRLWCKKKIEEG	3979.73	3979.8 $[M+3H]^{3+}$	13.8	9,261 ± 2,210	42,409 ± 10,010	6.2	[32]
GrTx I	YCQKWMWTCDSKRKCCEDMVCQLWCKKRL	3697.5	3698.4 $[M+3H]^{3+}$	17.8	1,007 ± 600	2,690 ± 460	2.7	[33]
PaTx I	YCQKWMWTCDSARKCCEGLVCRLWCKKII	3549.36	3548.7 $[M+3H]^{3+}$	12.6	423 ± 110	5000	10	[34]
GsMTx II/PaTX II	YCQKWMWTCDEERKCCEGLVCRLWCKRIINM	3922.75	3923.1 $[M+3H]^{3+}$	14.7	260 ± 50	2,699 ± 790	10.3	[35,36]

[a]Information also obtained from Uniprot (www.uniprot.org).
[b]Toxins have three disulfide bridges in Cys1–Cys4, Cys2–Cys5 and Cys3–Cys6; manner and functional group of C-terminus are COOH.
[c]10–60%B over 30 min.
[d]Selectivity for Nav1.7 over Nav1.2.

These characteristics of the protoxin II block are consistent with the majority of the current in these cells being mediated by Nav1.7 channels.

Synthesis of Other Inhibitory Cystine Knot Peptides and Biological Activity for Nav1.7 and Nav1.2

After successful synthesizing and confirming the biological activity of protoxin II, eight other natural inhibitory cystine knot peptides were selected and synthesized using the described methodology. These peptides were chosen because of their high homology to protoxin II. According to Table 1, these highly similar peptides display a large range of potencies on Nav 1.7 channels and degree of selectivity over Nav1.2 channels. Among these peptides, protoxin II had the highest potency on Nav1.7 channels and also demonstrated the largest selectivity over Nav1.2. GsAF II and VsTx II differ by only one amino acid (W31 → EG) in the terminal region but GsAF II displays approximately 130 times more potency against Nav1.7 than VsTx II but similar selectivity over Nav1.2 channels. These data indicate that the flexible tail region of these peptides may play an important role in determining the potency on VGSC activity and that W is more favored than EG. Currently, there are no clear data indicating which amino acids or part of the tertiary structure contributes to Nav1.7-selectivity.

Conclusions

Protoxin II, a member of the inhibitory cystine knot (ICK) family of peptides was synthesized and its function confirmed by electrophysiology. During linear synthesis, significant racemization was observed that could be suppressed by substituting base from NMM to 2,4,6-collidine and solvent from DMF to DCM/DMF (1 : 1). Racemization could reoccur by changing the base from 2,4,6-collidine back to NMM.

Eight other ICK toxins were synthesized with this same methodology and electrophysiological assessment of their biological activity against Nav1.7 and Nav1.2 channels are summarized. Among the nine peptides tested, protoxin II had the highest potency on Nav1.7 channels and greatest selectivity over Nav1.2 channels.

Acknowledgements

We would like to thank Laszlo Musza for providing the ICK toxin sequences. We would also like to thank G. Crumley for subcloning hNav1.5 and hNav1.7 recombinant cell lines and Dr. R. Kumar for subcloning ND7/23 cells.

References

1 Fischer TZ, Waxman SG. Familial pain syndromes from mutations of the NaV1.7 sodium channel. *Ann. N. Y. Acad. Sci.* 2010; **1184**: 196–207.
2 Herzog RI, Cummins TR, Ghassemi F, Dib-Hajj SD, Waxman SG. Distinct repriming and closed-state inactivation kinetics of Nav1.6 and Nav1.7 sodium channels in mouse spinal sensory neurons. *J. Physiol.* 2003; **551**: 741–750.
3 Choi JS, Waxman SG. Physiological interactions between Nav1.7 and Nav1.8 sodium channels: a computer simulation study. *J. Neurophysiol.* 2011; **106**: 3173–3184.
4 Nassar MA, Stirling LC, Forlani G, Baker MD, Matthews EA, Dickenson AH, Wood JN. Nociceptor-specific gene deletion reveals a major role for Nav1.7 (PN1) in acute and inflammatory pain. *Proc. Natl. Acad. Sci. U.S.A.* 2004; **101**: 12706–12711.
5 Cox JJ, Reimann F, Nicholas AK, Thornton G, Roberts E, Springell K, Karbani G, Jafri H, Mannan J, Raashid Y, Al-Gazali L, Hamamy H,

Valente EM, Gorman S, Williams R, McHale DP, Wood JN, Gribble FM, Woods CG. An SCN9A channelopathy causes congenital inability to experience pain. *Nature* 2006; **444**: 894–898.
6 Middleton RE, Warren VA, Kraus RL, Hwang JC, Liu CJ, Dai G, Brochu RM, Kohler MG, Gao YD, Garsky VM, Borusky MJ, Mehl JT, Cohen CJ, Smith MM. Two tarantula peptides inhibit activation of multiple sodium channels. *Biochemistry* 2002; **41**: 14734–14747.
7 Schmalhofer WA, Calhoun J, Burrows R, Bailey T, Kohler MG, Weinglass AB, Kaczorowski GJ, Garcia ML, Koltzenburg M, Priest BT. ProTx-II, a selective inhibitor of NaV1.7 sodium channels, blocks action potential propagation in nociceptors. *Mol. Pharmacol.* 2008; **74**: 1476–1484.
8 Pallaghy PK, Nielsen KJ, Craik DJ, Norton RS. A common structural motif incorporating a cystine knot and a triple-stranded beta-sheet in toxic and inhibitory polypeptides. *Protein Sci.* 1994; **10**: 1833–1839.
9 Angell Y, Han Y, Albericio F, Barany, G. Minimization of cysteine racemization during stepwise solid-phase peptide synthesis. In *Peptides: Frontiers of Peptide Science (Proceedings of the 15th American Peptide Symposium)*, Tam JP and Kaumaya PTP (eds.). Kluwer: Dordrecht, The Netherlands, 2002; 339–340.
10 Han Y, Albericio F, Barany G. Occurrence and minimization of cysteine racemization during stepwise solid-phase peptide synthesis. *J. Org. Chem.* 1997; **62**: 4307–4312.
11 Loidl G, Dick F, Mergler M, Schoenleber RO. Optimized coupling protocols for the incorporation of Cys derivatives during Fmoc-SPPS. *Adv. Exp. Med. Biol.* 2009; **611**: 163–164.
12 Angell YM, Alsina J, Baranu G, Albericio F. Practical protocols for stepwise solid-phase synthesis of cysteine-containing peptides. *J. Pept. Res.* 2002; **60**: 292–299.
13 Kaiser T, Nicholson GJ, Kohlbau HK, Voelter W. Racemization studies of Fmoc-Cys(Trt)-OH during stepwise Fmoc-solid phase peptide synthesis. *Tetrahedron Lett.* 1996; **37**: 1187–1190.
14 Musiol HJ, Siedler F, Quarzago D, Moroder L. Redox-active bis-cysteinyl peptides. I. Synthesis of cyclic cystinyl peptides by conventional methods in solution and on solid supports. *Biopolymers* 1994; **34**: 1553–1562.
15 Frare E, de Laureto PP, Scaramella E, Tonello F, Marin O, Deana R, Fontana A. Chemical synthesis of the RGD-protein decorsin: Pro → Ala replacement reduces protein thermostability. *Protein Eng. Des. Sel.* 2005; **18**: 487–495.
16 Wang I, Wu SH, Chang HK, Shieh RC, Yu HM, Chen C. Solution structure of a K^+-channel blocker from the scorpion. *Tityus cambridgei*. *Protein Sci.* 2002; **11**: 390–400.
17 Fajloun Z, Ferrat G, Carlieri E, Fathallah M, Lecomte C, Sandozi G, Luccio ED, Mabrouk K, Legros C, Darbon H, Rochat H, Sabatier JM, Waardi MD. Synthesis, ^{1}H NMR structure, and activity of a three-disulfide-bridged maurotoxin analog designed to restore the consensus motif of scorpion toxins. *J. Biol. Chem.* 2000; **275**: 13605–13612.
18 Savarin P, Romi-Lebrun R, Zinn-Justin S, Lebrun B, Nakajima T, Gilquin B, Menez A. Structural and functional consequences of the presence of a fourth disulfide bridge in the scorpion short toxins: solution structure of the potassium channel inhibitor HsTX1. *Protein Sci.* 1999; **8**: 2672–2685.
19 De-Laureto PP, Scaramella E, De Filippis V, Marin O, Doni MG, Fontana A. Chemical synthesis and structural characterization of the RGD-protein decorsin: a potent inhibitor of platelet aggregation. *Protein Sci.* 1998; **7**: 433–444.
20 Sabatier JM, Lecomte C, Mabrouk K, Darbon H, Oughideni R, Canarelli S, Rochat H, Martin-Eauclaire MF, van Rietschoten J. Synthesis and characterization of leiurotoxin I analogs lacking one disulfide bridge: evidence that disulfide pairing 3–21 is not required for full toxin activity. *Biochemistry* 1996; **35**: 10641–10647.
21 Juirou B, Mosbah A, Visan V, Grissmer S, M'Barek S, Fajloun Z, Van Rietschoten J, Devaux C, Rochat H, Lippens G, El Ayeb M, De Waard M, Mabrouk K, Sabatier JM. Cobatoxin 1 from Centruroides noxius scorpion venom: chemical synthesis, three-dimensional structure in solution, pharmacology and docking on K+ channels. *Biochem. J.* 2004; **377**: 37–49.
22 Zamborelli TJ, Dodson WS, Harding BJ, Zhang J, Bennett BD, Lenz DM, Young Y, Haniu M, Liu CF, Jones T, Jarosinski MA. A comparison of folding techniques in the chemical synthesis of the epidermal growth factor-like domain in neu differentiation factor alpha/beta. *J. Pept. Res.* 2000; **55**: 359–371.
23 Smith JJ, Cummins TR, Alphy S, Blumenthal KM. Molecular interactions of the gating modifier toxin ProTx-II with NaV1.5: implied existence of a novel toxin binding site coupled to activation. *J. Biol. Chem.* 2007; **282**: 12687–12697.
24 Steiner AM, Bulaj G. Optimization of oxidative folding methods for cysteine-rich peptides: a study of conotoxins containing three disulfide bridges. *J. Pept. Sci.* 2011; **17**: 1–7.
25 Edgerton GB, Blumenthal KM, Hanck DA. Evidence for multiple effects of ProTxII on activation gating in Na(V)1.5. *Toxicon* 2008; **52**: 489–500.
26 Sokolov S, Kraus RL, Scheuer T, Catterall WA. Inhibition of sodium channel gating by trapping the domain II voltage sensor with protoxin II. *Mol. Pharmacol.* 2008; **73**: 1020–1028.
27 Xiao Y, Blumenthal K, Jackson JO 2nd, Liang S. Cummins TR. The tarantula toxins ProTx-II and huwentoxin-IV differentially interact with human Nav1.7 voltage sensors to inhibit channel activation and inactivation. *Mol. Pharmacol.* 2010; **78**: 1124–1134.
28 Zeng XZ, Deng M, Lin Y, Yuan C, Pi J, Liang SP. Isolation and characterization of Jingzhaotoxin-V, a novel neurotoxin from the venom of the spider Chilobrachys jingzhao. *Toxicon* 2007; **49**: 388–399. DOI: dx.doi.org
29 Yuan C, Liao Z, Zeng X, Dai L, Kuang F, Liang S. Jingzhaotoxin-XII, a gating modifier specific for Kv4.1 channels. *Toxicon* 2007; **50**: 646–652.
30 Lampe RA. U.S. Patent 5877026, 1999.
31 Lampe RA, Sachs F. U.S. Patent 5968838, 1999.
32 Ruta V, MacKinnon R. Localization of the voltage-sensor toxin receptor on KvAP. *Biochemistry* 2004; **43**: 10071–10079.
33 Clement H, Odell G, Zamudio FZ, Redaelli E, Wanke E, Alagon A, Possani LD. Isolation and characterization of a novel toxin from the venom of the spider Grammostola rosea that blocks sodium channels. *Toxicon* 2007; **50**: 65–74.
34 Chagot B, Escoubas P, Villegas E, Bernard C, Ferrat G, Corzo G, Lazdunski M, Darbon H. Solution structure of Phrixotoxin 1, a specific peptide inhibitor of Kv4 potassium channels from the venom of the theraphosid spider Phrixotrichus auratus. *Protein Sci.* 2004; **13**: 1197–1208.
35 Oswald RE, Suchyna TM, McFeeters R, Gottlieb PA, Sachs F. Solution structure of peptide toxins that block mechanosensitive ion channels. *J. Biol. Chem.* 2002; **277**: 34443–34450.
36 Diochot S, Drici MD, Moinier D, Fink M, Lazdunski M. Effects of phrixotoxins on the Kv4 family of potassium channels and implications for the role of Ito1 in cardiac electrogenesis. *Br. J. Pharmacol.* 1999; **126**: 251–263.

